

Shape of Power Spectrum of Intermittent Chaos*

B.C. So and H. Mori

Department of Physics
Kyushu University
Fukuoka 33, Japan

Abstract

Power spectra of intermittent chaos are calculated analytically. It is found that the power spectrum near onset point consists of a large number of Lorentzian lines with two peaks around frequencies $\omega = 0$ and $\omega = \omega_0$, where ω_0 is a fundamental frequency of a periodic orbit before the onset point, and furthermore the envelope of lines around $\omega = 0$ obeys the power law $1/|\omega|^2$, whereas the envelope around ω_0 obeys $1/|\omega - \omega_0|^4$.

The universality of these power law dependence in a certain class of intermittent chaos are clarified from a phenomenological view point.

* Presented at the US-Japan Workshop on Statistical Plasma Physics, February, 1984, Nagoya, Japan.

1. Introduction

How can we recognize a given time record to be chaotic? The power spectrum of a time record gives us the information such that how many oscillations are involved in the time record. Thus it is natural to define a given time record to be chaotic if the power spectrum has a continuous broad band component. Furthermore, the power spectrum exhibits a measure-theoretical structure of orbits in phase space. Therefore the shape of power spectrum is a fundamental quantity to analyze the structure and the growth of chaos.

In section 2, we review a method for calculating the time correlation and the power spectrum in terms of the Perron-Frobenius operator. In section 3, the power spectra of two different onset types of intermittent chaos generated by one-dimensional maps are calculated. In section 4, a phenomenological theory for shapes of the power spectrum of intermittent chaos is discussed.

2. Analytic method for calculating the power spectrum⁽¹⁾

Let us consider an orbit $\{x_i\}$ generated by a one-dimensional map $f(x)$:

$$x_{i+1} = f(x_i) = f^i(x_0) , \quad (2.1)$$

where $f^i(x) = f \circ f^{i-1}(x)$. Let us assume $f(x)$ is ergodic in the unite interval $I = (0,1)$. Then, for almost all initial point x_0 , the orbit $\{x_i\}$ covers I densely so that the long-time average of a function $g(x)$ can be replace by the space average as

$$\lim_{N \rightarrow \infty} \frac{1}{N} \sum_{i=0}^N g(x_i) = \int_0^1 dx P^* x g(x) \equiv \langle g(x) \rangle , \quad (2.2)$$

where $P^* x$ is the invariant density of the map f . The invariant

density satisfies $\{H P^*\}(x) = P^*(x)$ in terms of the Perron-Frobenius operator H ,

$$\{H g\}(x) \equiv \int_0^1 dy \delta(x-f(y))g(y) = \sum_i g(y_i)/|f'(y_i)|. \quad (2.3)$$

Then, the time correlation function of orbits C_t can be written as

$$C_t = \int_0^1 dx f^t(x)P^*(x)\delta x = \int_0^1 dx x H^t\{P^*(x)\delta x\}, \quad (2.4)$$

where $\delta x \equiv x - \langle x \rangle$. The power spectrum $S(\omega)$ is given by

$$S(\omega) = \sum_{t=-\infty}^{\infty} C_t \exp(-i\omega t), \quad (C_{-t} \equiv C_t). \quad (2.5)$$

If we can expand $P^*(x)\delta x$ in terms of the eigenfunctions $\{\psi_j\}$ of H , $H \psi_j = \nu_j \psi_j$, as

$$P^*(x)\delta x = \sum_j b_j \psi_j, \quad (2.6)$$

then we obtain

$$C_t = \sum_j B_j \nu_j^t, \quad B_j \equiv b_j \int_0^1 dx x \psi_j(x), \quad (2.7)$$

$$S(\omega) = \sum_j B_j / \{1 - \nu_j \exp(-i\omega)\} + c.c. - 1. \quad (2.8)$$

Therefore, the power spectrum consists of Lorentzian spectral lines at frequencies $\omega = \omega_j$ with widths $\gamma_j = -\ln|\nu_j|$, where $\nu_j = |\nu_j| \exp(i\omega_j) = \exp(-\gamma_j + i\omega_j)$.

Thus, if one can find the eigenfunction expansion (2.6), then one

can study the time correlation function and power spectrum analytically.

Before the onset of intermittent chaos, the power spectrum consists of a single line with zero width, representing a stable periodic orbit. After the onset, the power spectrum consists of a number of Lorentzian lines and the shape of the power spectrum critically depends on whether the separation $\Delta\omega_i \equiv \omega_{i+1} - \omega_i$ is larger than the width γ_i , or not. Which case occurs depends on the mechanism of chaos, the excitation parameter and the external noise.

3. Two types of intermittent chaos 2.4

There may exist several types of the onset of intermittent chaos. We shall discuss two types. One type (Type A) is an abrupt excitation of an infinite number of unstable periodic orbits. The other (Type B) is a collapse of a pair of stable and unstable periodic orbits. Simple maps which exhibit these two types are the map f_A and f_B shown in Fig.1 and Fig.2, respectively. If a map is piecewise linear and satisfies the finite Markov condition, then the power spectrum of the map can be calculated analytically with the use of the Perron-Frobenius operator as explained in section 2. This is the technical reason why we take piecewise linear maps.

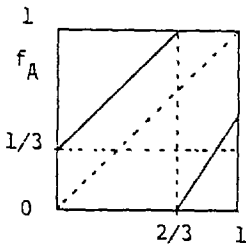


Fig.1 $f_A(x)$

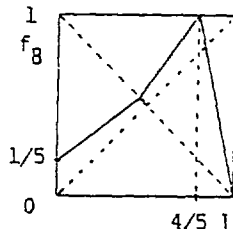


Fig.2 $f_B(x)$

$$f_A(x) = \begin{cases} x + (1/3) & 0 \leq x \leq 2/3 \\ \beta(x - (2/3)) & 2/3 < x \leq 1 \end{cases}$$

$$f_B(x) = \begin{cases} \beta x + (1/5) & 0 \leq x < c \\ \beta^{-1}x + \beta^{-1}(\beta - (4/5)) & c \leq x < 4/5 \\ 5(1-x) & 4/5 < x \leq 1 \end{cases}$$

$$c = 0.8 / (1 + \beta)$$

β : parameter

Figures 3 and 4 show orbits of these maps at several excitation parameter values.

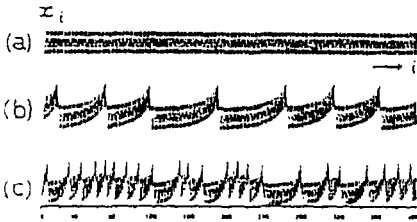


Fig.3 Orbit $\{x_i\}$ of the map f_A :
 (a) $\beta < 1$ (b) $\beta = 1.114465$ (c) $\beta = 1.324718$

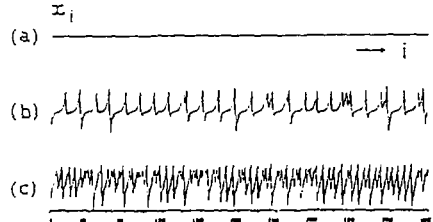


Fig.4 Orbit $\{x_i\}$ of the map f_B :
 (a) $\beta < 0.6$ (b) $\beta = 0.605$ (c) $\beta = 0.75$

Comparison between Type A and Type B .

Figures 5 and 6 show the invariant density of the maps f_A and f_B , respectively. The invariant density of f_B has a single peak at the center of a narrow channel, whereas the invariant density of f_A has three peaks at the periodic cycle of period 3.

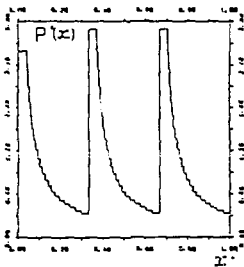


Fig.5 Invariant density of the map f_A at $\beta = 1.114465$

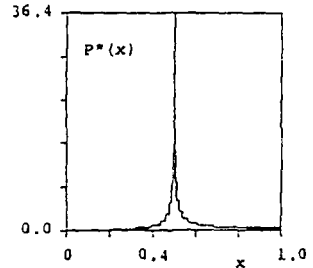


Fig.6 Invariant density of the map f_B at $\beta = 0.602003$

Figures 7 and 8 show the power spectra of the maps f_A and f_B , respectively. Analyzing the exact expression for the power spectra, we obtain following results.

(1) The power spectra of the maps f_A and f_B consist of a large number of Lorentzian lines as shown in Figs. 7 and 8. The number of lines blows up in both maps, as the excitation parameter decreases to the onset points.

(2) In the vicinity of the onset point, the power spectrum has the highest Lorentzian line around frequency ω_0 , where ω_0 is the fundamental frequency of the periodic state before the onset of chaos.

(3) Figure 7(c) for the map f_A has two dominant peaks; the highest peak locates around $\omega_0 = 2\pi/3$ with an envelope of the power law $1/|\omega-\omega_0|^4$, and the second-highest peak locates around $\omega = 0$ with an envelope $1/|\omega|^2$. On the other hand, Fig.8(c) for f_B has one dominant peak around $\omega = 0$ and its envelope obeys the power law $1/|\omega|^2$. It should be noted that the power laws for the envelope are the asymptotic behavior in the vicinity of the onset point. Their exponents, 4 and 2, can be shown to be universal irrespective of details of the models.

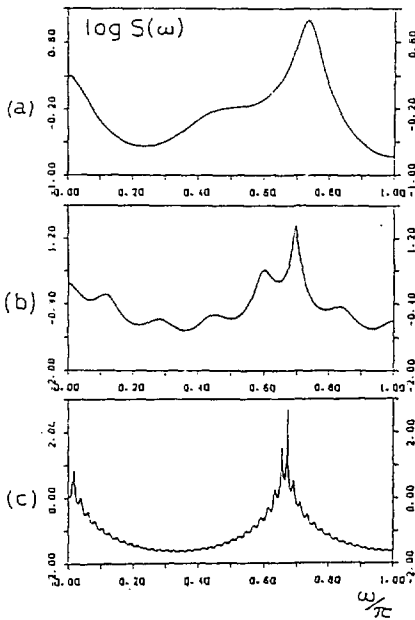


Fig.7 Power spectrum of the map f_A :
 (a) $\beta = 1.618034$ (b) $\beta = 1.324718$
 (c) $\beta = 1.085450$

The onset point is $\beta = 1$.

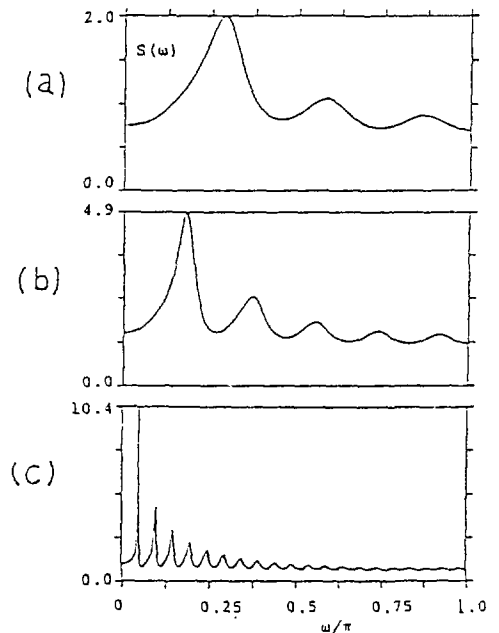


Fig.8 Power spectrum of the map f_B :
 (a) $\beta = 0.742959$ (b) $\beta = 0.633268$
 (c) $\beta = 0.600012$

The onset point is $\beta = 0.6$.

(4) The highest Lorentzian line around ω_0 determines the most important feature of the time correlation function, which exhibits an interesting behavior when $\omega_0 \neq 0$. We consider the case $\omega_0 \neq 0$. Let $\omega_L = \omega_0(1 + \hat{q})$ and γ_L be the frequency and the width of the highest line, respectively, where \hat{q} represents the misfit of the frequency. Figure 7(c) has $\omega_0 = 2\pi/3$ and $\hat{q} = 0.008019$, $\gamma_L = 0.0013637$. Figure 9 shows the time correlation functions which corresponds to the power spectra in Fig.7. The time correlation consists of a rapid oscillation with period 3 and a slow oscillation of the amplitude with period about 125.

The period 3 represents the frequency ω_0 , whereas the long period 125 arises from the misfits \hat{q} . Indeed $T_{amp} = 1/\hat{q} = 124.7$. The damping constant of the time correlation is given by γ_L .

4. Phenomenological theory of power spectrum of intermittent chaos.³⁾

Let us take the onset of intermittent chaos from a periodic state. Let $X(t)$ be a time record. Before the onset, $X(t)$ is periodic in time with a fundamental frequency ω_0 so that $X(t) = \exp(i\omega_0 t)$. After the onset, $X(t)$ takes the form

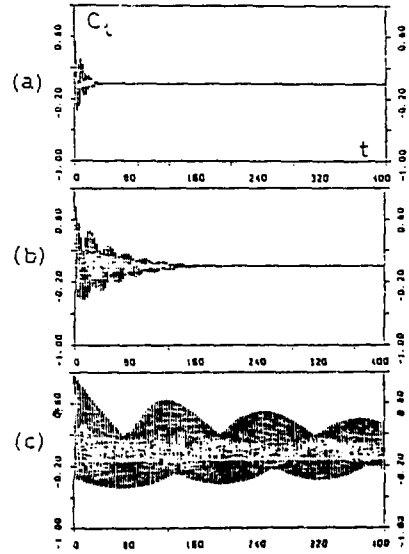


Fig.9 Time-correlation function C_t of the map f_A : (a) $\beta = 1.618034$
 (b) $\beta = 1.324718$ (c) $\beta = 1.085450$

$$X(t) = \{1 + b(t)\} \exp[i\omega_0 t + i\phi(t)], \quad (4.1)$$

where $b(t)$ and $\phi(t)$ represent the amplitude modulation and the phase modulation at time t , respectively.

Let us suppose that there are m bursts in a long time interval $2T$, and the n -th burst locates in a short time interval $[T_n, T_n + \tau_c]$, where τ_c is the mean lifetime of one burst. The laminar state between the n -th and $n+1$ -th burst is called the n -th laminar state. The mean recurrence time of bursts is given by $\bar{\tau} \equiv \langle \tau_n \rangle$, where $\tau_n \equiv T_{n+1} - T_n$. As the onset point is approached, $\bar{\tau}$ becomes infinity. Hence we may assume $\bar{\tau} \gg \tau_c$ near the onset point. Then $\bar{\tau}$ also represents the mean duration time of laminar states. Then the spectrum can be written as

$$S(\omega) \equiv \lim_{T \rightarrow \infty} \frac{1}{2T} \int_{-T}^T dt \int_{-t}^T dt' \langle X(t) X(t') \exp(-i\omega(t-t')) \rangle, \quad (4.2)$$

$$= \lim_{m \rightarrow \infty} \frac{1}{2T} \sum_{n=1}^m \sum_{n'=1}^m \langle \exp(-i\omega(T_n - T_{n'})) \int_0^{\tau_n} dt \int_0^{\tau_{n'}} dt' X_n(t) X_{n'}(t') \exp(-i\omega(t-t')) \rangle, \quad (4.3)$$

where $2T = \sum_{n=1}^m \tau_n = m\bar{\tau}$ and we have defined

$$X_n(t) \equiv \{1 + b_n(t)\} \exp(i\omega_0 T_n) \exp(i\omega_0 t + i\phi_n) \quad (4.4)$$

for the time interval $[T_n + \tau_c, T_{n+1}]$, with $b_n(t)$ and ϕ_n being the amplitude and the phase modulation of the n -th laminar state, respectively.

Which of ϕ_n or $b_n(t)$ gives a more important contribution depends on the mechanism of intermittency and the frequency region of interest.

A. Bursts in phase

Let us first consider the contribution of φ_n , neglecting $b_n(t)$. This is valid as far as $\omega_0 \neq 0$ and the frequency region around ω_0 is concerned with.

The phase φ_n is changed by bursts randomly. Thus we are left with two random variables τ_n and $\xi_n \equiv \varphi_n - \varphi_{n-1}$, where ξ_n is a phase jump caused by the n -th burst. The mean phase jump is given by $\bar{\xi} \equiv \langle \xi_n \rangle$. We assume that bursts at different times are statistically independent of each other. Therefore any two of ξ_n 's and τ_n 's with different n are statistically independent of each other, and also ξ_n and τ_n are statistically independent of each other. Under these assumptions, we obtain

$$S(\omega) = (2/\bar{\tau}\omega^2) F(\omega) , \quad (4.5)$$

$$F(\omega) \equiv \frac{e^{2(\eta^2+\gamma)} - 1 - e^\gamma \{e^{2\eta^2} - 1\} \cos(\omega\tau) + e^{\eta^2} \{1 - e^{2\gamma}\} \cos\xi}{e^{2(\eta^2+\gamma)} + 1 - 2e^{(\eta^2+\gamma)} \cos(\omega\tau - \xi)} \quad (4.6)$$

where $\omega - \omega_0$ has been denoted by ω , and $\tau, \gamma, \xi, \eta^2$ are real quantities defined by

$$\langle \exp(-i\omega\tau_n) \rangle = \exp(-i\omega\tau - \gamma) , \quad (4.7a)$$

$$\langle \exp(i\xi_n) \rangle = \exp(i\xi - \eta^2) . \quad (4.7b)$$

If τ_n and ξ_n are Gaussian random variables, then (4.7) leads to

$$\tau = \bar{\tau}, \quad \gamma = \omega^2 \sigma^2 / 2, \quad \sigma^2 \equiv \langle (\tau_n - \bar{\tau})^2 \rangle , \quad (4.8a)$$

$$\xi = \bar{\xi}, \quad \eta^2 = \langle (\xi_n - \bar{\xi})^2 \rangle / 2 . \quad (4.8b)$$

In the present paper, we do not assume this Gaussian statistics.

However, (4.8a) is valid for small frequencies $\omega^2 \ll 2/\sigma^2$.

The function $F(\omega)$ takes different forms, depending on the magnitudes of γ and η^2 . They can be classified into following three types.

$$\underline{[A1] \quad \gamma \gg 1.}$$

Then (4.5) reduces to

$$S(\omega) \simeq (2/\tau\omega^2)\{1 - \exp(-\eta^2)\cos(\xi)\}. \quad (4.9)$$

This is valid for large frequencies $\omega^2 \gg 2/\sigma^2$. Therefore the power spectrum has a tail which decays as $1/\omega^2$.

$$\underline{[A2] \quad \eta^2 \ll 1, \quad \gamma \simeq \omega^2\sigma^2/2 \ll 1.}$$

Then (4.5) reduces to

$$S(\omega) = \sum_k S_k(\omega) + S_B(\omega), \quad (4.10)$$

where

$$S_k(\omega) = \frac{2(1-\cos\xi)}{(\tau\omega_k)^2} \frac{\Gamma_k}{\Gamma_k^2 + (\omega_k - \omega)^2} : \text{Lorentzian spectral line} \quad (4.11)$$

$$\omega_k \equiv \{\xi + 2\pi(k-1)\}/\tau, \quad (k=1,2,3,\dots) \quad (4.12)$$

$$\Gamma_k \equiv \{\eta^2 + \omega_k^2\sigma^2/2\}/\tau, \quad (4.13)$$

and $S_B(\omega)$ is a background spectrum.

Equation (4.15) leads to two different cases, depending on the relative magnitude of η^2 and γ .

$$\underline{[A2(a)] \quad \eta^2 \ll \gamma, \text{ i.e., } \omega_k^2 \gg 2\eta^2/\sigma^2.}$$

Then (4.12) and (4.11) lead to

$$\Gamma_k \simeq \omega_k^2\sigma^2/2\tau, \quad S_k(\omega_k) \simeq 1/\omega_k^4. \quad (4.14)$$

Hence the line width depends on frequency as ω^2 , and the envelope of the spectral lines obeys the power law $1/\omega^4$. If $\eta \simeq 0$, then this holds down to $\omega \simeq 0$. Indeed, the map $f_A(x)$ in section 2 is such an example.

$$\text{(A2(b)) } \eta^2 \gg \gamma, \text{ i.e., } \omega_k^2 \ll 2\eta^2/\sigma^2.$$

This is satisfied by several small k 's if $\sigma/\tau \ll \eta/\sqrt{2\pi}$. Then (4.12) and (4.11) lead to

$$\Gamma_k \simeq \eta^2/\tau, \quad S_k(\omega_k) \simeq 1/\omega_k^2. \quad (4.15)$$

Hence the envelope of the spectral lines obeys the power law $1/\omega^2$.

$$\text{(A3) } \eta^2 \gg 1.$$

Then (4.5) reduces to

$$S(\omega) \simeq (2/\tau\omega^2)(1 - \exp(-\gamma)\cos(\omega\tau)). \quad (4.16)$$

Therefore $S(\omega) \simeq S(0)\{1 - c\omega^2\}$ for $|\omega| \ll 2/\sigma$, $\Delta\omega$ with a positive constant c , and the power spectrum has a broad peak around $\omega \simeq 0$, as shown in Fig.10. This is due to the fact that spectral lines around $\omega \simeq 0$ are amalgamated to produce one smooth broad peak.

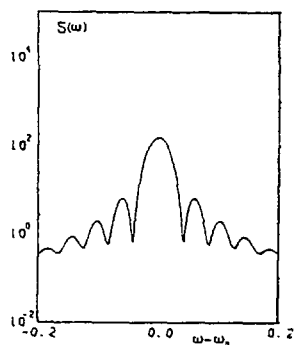


Fig. 10 $S(\omega)$ vs ω around ω_0 in the case of $\eta^2 \gg 1$ with $\eta = 10$, $\tau = 150$, $\sigma = 10$, $\xi = 2\pi/3$.

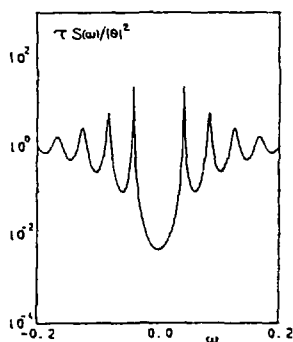


Fig. 11 $S(\omega)$ vs ω around $\omega = 0$ with $\tau = 150$, $\sigma = 10$. This is obtained from (4.22) with $\Upsilon(\omega) = \omega^2\sigma^2/2$.

B. Bursts in amplitude

Let us next consider the contribution of $b_n(t)$ of (4.4), putting $\omega_0 = \varphi_n = 0$. This is valid for the intermittent chaos developed from a steady state. Even when $\omega_0 \neq 0$, this would be valid for a small frequency region around $\omega = 0$.

Then, in a similar way as before, (4.3) can be reduced to

$$S(\omega) = \frac{1}{\tau} |\theta(\omega)|^2 \left\{ \zeta - \frac{\mu(1-e^{\lambda\tau}) + (1-e^{-\lambda\tau})}{e^{\lambda\tau} + 1 - |e^{\lambda\tau} + e^{-\lambda\tau}|} \right\} \quad (4.17)$$

where

$$\theta(\omega) \equiv \int_0^\tau dt \exp(-i\omega t) \langle b_n(t) \rangle \quad (4.18)$$

and we have defined ζ , μ , and λ by

$$\left\langle \int_0^{\tau_n} dt \int_0^{\tau_n} dt' e^{-i\omega(t-t')} b_n(t) b_n(t') \right\rangle = |\theta(\omega)|^2 \zeta, \quad (4.19)$$

$$\langle e^{-i\omega\tau_n} \rangle = e^{-i\omega\tau - \gamma} \equiv e^{-\lambda}, \quad (4.20)$$

$$\langle e^{-i\omega\tau_n} \int_0^{\tau_n} dt b_n^*(t) e^{i\omega t} \rangle = e^{-\lambda} \theta^*(\omega) \mu. \quad (4.21)$$

As the first approximation, we take $\zeta=1$, $\mu=1$. Then (4.17) reduced to

$$S(\omega) \simeq \frac{1}{\tau} |\theta(\omega)|^2 \frac{1 - e^{-2\gamma}}{1 - 2e^{-\gamma} \cos(\omega\tau) + e^{-2\gamma}}. \quad (4.22)$$

One example of (4.22) is shown in Fig.11, where $|\theta(\omega)|^2$ may be assumed to be constant in a small frequency region around $\omega = 0$.

Near the onset point, the spectrum (4.22) consists of a number of

Lorentzian lines in a small frequency region where $\omega^2 \ll 2\sigma^2$. Then we have (4.10) with the Lorentzian lines

$$S_k(\omega) \simeq \frac{2}{\tau^2} |\theta(\omega_k)|^2 \frac{\Gamma_k}{\Gamma_k^2 + (\omega_k - \omega)^2} \quad (4.23)$$

for $|\omega - \omega_k| \ll \Delta\omega$, where $\omega_k \equiv 2\pi/\tau$, ($k=1,2,3,\dots$),

$$\Gamma_k \equiv \frac{2}{\tau} \sinh(\gamma(\omega_k)/2) \simeq \omega_k^2 \sigma^2 / 2\tau. \quad (4.24)$$

If $|\theta(\omega)|^2$ is nearly constant, then (4.23) leads to the power law envelope of $1/\omega^2$. Indeed, the map $f_B(x)$ in section 2 is such an example.

References

1. H.Mori, B.C.So and T.Ose : Prog.Theor.Phys.66,1266(1981)
H.Shigematsu, H.Mori, T.Yoshida and H.Okamoto :
J.Stat.Phys.30,649(1983)
T.Yoshida, H.Mori and H.Shigematsu : J.Stat.Phys.31,279(1983)
2. B.C.So, N.Yoshitake, H.Okamoto and H.Mori : "Correlations and Spectra of an Intermittent Chaos near its onset Point" J.Stat.Phys.36(1984)(to appear)
3. K.Shobu, T.Ose and H.Mori : "Shapes of the Power Spectrum of Intermittent Turbulence near its Onset Point" (to be submitted to Prog.Theor.Phys.)
4. B.C.So and H.Mori : "Analytic Study of Power Spectra of Intermittent Chaos" (to appear in Chaos and Statistical Mechanics, Springer, ed. Y. Kuramoto.)